

Fitness Landscape Analysis of a Cell-Based Neural Architecture Search Space

Devon Tao^a and Lucas Bang^b

Computer Science Department, Harvey Mudd College, Claremont, CA, U.S.A.
{vtao, lbang}@hmc.edu

Keywords: Neural Architecture Search, Fitness Landscape, Neural Networks.

Abstract: Neural Architecture Search (NAS) research has historically faced issues of reproducibility and comparability of algorithms. To address these problems, researchers have created NAS benchmarks for NAS algorithm evaluation. However, NAS search spaces themselves are not yet well understood. To contribute to an understanding of NAS search spaces, we use the framework of *fitness landscape analysis* to analyze the topology search space of NATS-Bench, a popular cell-based NAS benchmark. We examine features of *density of states*, *local optima*, *fitness distance correlation* (FDC), *fitness distance rank correlations*, *basins of attraction*, *neutral networks*, and *autocorrelation* in order to characterize the difficulty and describe the shape of the NATS-Bench topology search space on CIFAR-10, CIFAR-100, and ImageNet16-120 image classification problems. Our analyses show that the difficulties associated with each fitness landscape could correspond to the difficulties of the image classification problems themselves. Furthermore, we demonstrate the importance of using multiple metrics for a nuanced understanding of an NAS fitness landscape.


1 INTRODUCTION


Neural networks have performed well in tasks such as image classification (He et al., 2016; Krizhevsky et al., 2012), speech recognition (Abdel-Hamid et al., 2014), and object detection (Szegedy et al., 2013). However, achieving state-of-the-art performance has traditionally required expert knowledge of neural architecture design. This poses a challenge for non-computer scientists who wish to use neural networks but lack the specific neural network expertise (Sheikhtaheri et al., 2014). One recent solution is Neural Architecture Search (NAS), where a neural architecture is algorithmically engineered as opposed to hand-designed. NAS has shown to be an effective architecture design method, in some cases outperforming hand-designed architectures (Zoph and Le, 2016).

While NAS has achieved state-of-the-art performance, it has also faced reproducibility issues due to algorithmic complexity and expensive computation (Li and Talwalkar, 2020). Furthermore, differences in training procedures and search spaces make it difficult to compare across methods (Ying et al., 2019). To combat these problems, researchers have created

NAS benchmarks, which provide common baselines for comparing algorithms and significantly reduce the costs of NAS evaluation (Ying et al., 2019; Dong and Yang, 2020; Siems et al., 2020). One popular benchmark is NATS-Bench, a cell-based NAS search space (Dong et al., 2021).

Although there have been analyses of NAS search spaces as a whole (White et al., 2023; Chitty-Venkata et al., 2023), there currently do not exist many deep analyses of specific NAS search spaces. While NAS algorithms have performed well on these spaces (Mellor et al., 2021; Chen et al., 2021), there is a lack of understanding of the search spaces themselves. We aim to fill this gap by analyzing the NATS-Bench topology search space through the framework of *fitness landscape analysis*, a concept originating from biology (Wright et al., 1932) that has since been applied to optimization problems (Merz and Freisleben, 2000; Tavares et al., 2008). We examine fitness landscape components of *density of states*, *local optima*, *fitness distance correlation* (FDC), *fitness distance rank correlations*, *basins of attraction*, *neutral networks*, and *autocorrelation* in order to characterize the difficulty of the NATS-Bench topology search space on three popular image classification datasets CIFAR-10, CIFAR-100 (Krizhevsky and Hinton, 2009), and ImageNet16-120, which is a

^a  <https://orcid.org/0009-0003-0507-0489>

^b  <https://orcid.org/0000-0003-2711-5548>

downsampled version of ImageNet (Chrabaszcz et al., 2017). We summarize our contributions as follows:

- We build upon previous NATS-Bench analyses (Ochoa and Veerapen, 2022; Thomson et al., 2023) by analyzing the fitness landscapes of the NATS-Bench topology search space test accuracies.
- We calculate and analyze several components of the NATS-Bench topology fitness landscape, augmenting previous NATS-Bench analyses of density of states, Spearman fitness distance correlation, and local optima networks (Ochoa and Veerapen, 2022) with additional characteristics of Pearson’s fitness distance correlation, basins of attraction, neutral networks, and autocorrelation. To our best knowledge, we are the first to calculate these metrics for the NATS-Bench topology search space. Due to the complexity of fitness landscapes, it is important to analyze many different metrics in order to create a deeper understanding of the fitness landscape (Pitzer and Affenzeller, 2012). To that end, the inclusion of these additional metrics reveals novel insights into the NATS-Bench topology search space.

2 RELATED WORK

The first NAS method used reinforcement learning (Zoph and Le, 2016). Since then, researchers have developed a variety of approaches, such as neuroevolution (Stanley et al., 2019), differentiable architecture search (Liu et al., 2018), one-shot NAS (Dong and Yang, 2019; Guo et al., 2020), and training-free methods (Mellor et al., 2021; Chen et al., 2021).

As for the search spaces themselves, there have been a number of established benchmarks for image classification problems such as NAS-Bench-101 (Ying et al., 2019), NAS-Bench-201 (Dong and Yang, 2020), NAS-Bench-301 (Siems et al., 2020), and NATS-Bench (Dong et al., 2021). More recently, there have also been NAS benchmarks in other areas such as automated speech recognition (Mehrotra et al., 2020) and natural language processing (Klyuchnikov et al., 2022).

Prior fitness landscape analyses of NAS search spaces include analyses of local optima networks (Potgieter et al., 2022; Rodrigues et al., 2022), FDC (Rodrigues et al., 2022), autocorrelation, entropic measure of ruggedness, fitness clouds, density clouds, and overfitting (Rodrigues et al., 2020). There additionally exist some analyses for specific benchmark datasets. The authors of NAS-Bench-101 analyze the FDC, locality, and autocorrelation of their benchmark

(Ying et al., 2019). Traoré et al. expand on this work with additional characteristics of ruggedness, cardinality of optima, and persistence (Traoré et al., 2021).

A few studies have examined the NATS-Bench benchmark specifically. Thomson et al. examine the local optima networks of the NATS-Bench size search space (Thomson et al., 2023) and Ochoa and Veerapen analyze the density of states, Spearman fitness distance correlation, and local optima networks of the NATS-Bench topology search space (Ochoa and Veerapen, 2022).

We expand on Ochoa and Veerapen’s work by analyzing the test accuracies rather than the validation accuracies of the NATS-Bench topology search space and by providing additional analyses. In addition to the Spearman correlation coefficient between fitnesses and distances, we also include Kendall and Pearson correlation coefficients. Notably, the Pearson correlation coefficient is the most established correlation coefficient in the literature (Jones et al., 1995), but it is missing from Ochoa and Veerapen’s analysis.¹ Moreover, Ochoa and Veerapen’s analysis focuses on local optima, whereas our analysis also provides insight into neutral areas. Furthermore, Ochoa and Veerapen’s analysis of ruggedness is entirely informed by the number of modes, while we provide an additional perspective by including autocorrelation. Overall, we corroborate Ochoa and Veerapen’s existing analyses while also providing a more nuanced understanding with additional metrics.

3 BACKGROUND

In this section, we introduce NATS-Bench, a repeated cell-based neural architecture search space. We then define a fitness landscape and its components and describe the specific fitness landscapes for the NATS-Bench topology search space.

3.1 NATS-Bench

NATS-Bench is a repeated-cell neural architecture benchmark that consists of a size search space \mathcal{S}_s and a topology search space \mathcal{S}_t (Dong et al., 2021). We analyze the topology search space \mathcal{S}_t , which is the same as NAS-Bench-201 (Dong and Yang, 2020). The macro structure of each neural architecture begins with a 3-by-3 convolution with 16 output channels and a batch normalization layer. It is then fol-

¹We note that Ochoa and Veerapen use “FDC” to refer to Spearman’s correlation coefficient, however the traditional use of “FDC” in the literature refers to Pearson’s correlation coefficient (Jones et al., 1995)

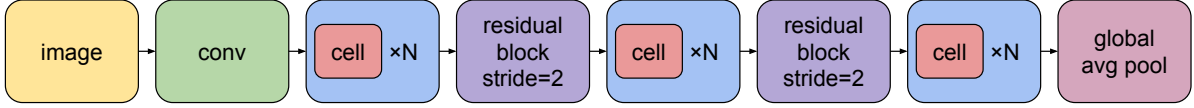


Figure 1: Macro structure of a neural architecture in the topology search space of NATS-Bench. Visual based on original paper (Dong et al., 2021).

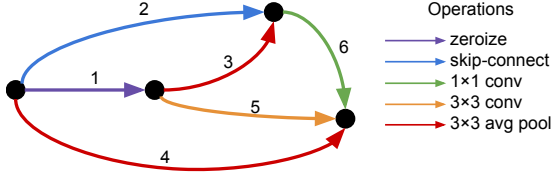


Figure 2: DAG representation of an individual cell. Visual based on original paper (Dong et al., 2021).

lowed by three stacks of $N = 5$ cells with a residual block between each cell stack. The number of output channels are 16, 32, and 64 for the three stacks respectively. These cell stacks are then followed by a global average pooling layer. The NATS-Bench architectures are trained on CIFAR-10, CIFAR-100, and ImageNet16-120, which is a downsampled version of ImageNet. Performance data for architectures in \mathcal{S}_t trained on 12 or 200 epochs of data can be accessed via the NATS-Bench API.² Further, architectures undergo many trials. For our analysis, our fitness values are the test accuracies of architectures trained on 200 epochs of data, averaging over all trials.

Each cell in \mathcal{S}_t can be represented as a densely-connected DAG with four vertices, where there is an edge from the i th node to the j th node if $i < j$ for a total of six edges. Each edge is selected from one of five operations: zeroize, skip connection, 1-by-1 convolution, 3-by-3 convolution, and 3-by-3 average pooling layer, where the zeroize operation represents dropping the edge. Then, there are $5^6 = 15625$ total architectures. However, some architectures are isomorphic, so there are only 6466 unique architectures (Dong and Yang, 2020).

3.2 Fitness Landscape Analysis

3.2.1 Definition

We use the definition of fitness landscape provided by Pitzer and Affenzeller (Pitzer and Affenzeller, 2012). There is a solution space \mathbf{S} and an encoding of the solution space \mathcal{S} . There is also a fitness function $f: \mathcal{S} \rightarrow \mathbb{R}$ that assigns a real-valued number to a solution candidate, and a distance metric $d: \mathcal{S} \times \mathcal{S} \rightarrow \mathbb{R}$.

Then, a fitness landscape is defined as the tuple

$$\mathcal{F} = (\mathcal{S}, f, d). \quad (1)$$

3.2.2 Fitness Landscape of NATS-Bench Topology Search Space

Each architecture in the NATS-Bench topology search space can be represented as a string of length six where each character represents an edge operation for a corresponding edge in the DAG representation of the cell. Then for \mathcal{S}_t , \mathcal{S} is the set of all possible neural architecture string representations. The distance function d is the Hamming distance between two such strings. We define the *neighborhood* of a solution candidate as $\mathcal{N}(x) = \{y \in \mathcal{S} | d(x, y) = 1\}$, that is, the set of architecture strings that represent a change of one edge operation from the architecture of x . We have three fitness functions, corresponding to average test accuracies of architectures trained on 200 epochs of data on CIFAR-10, CIFAR-100, and ImageNet16-120. Thus, we have three fitness landscapes, one for each image classification dataset.

For the purposes of analysis on NATS-Bench, we deviate from Pitzer and Affenzeller’s definitions of phenotype and genotype. Because some architectures are isomorphic, in addition to the string representation of the architecture, each architecture also has a string representation of the unique isomorph. We consider the string representation of the architecture the *genotype*, and the string representation of the unique isomorph the *phenotype*. Due to numerical error, two architectures with the same phenotype may have different fitnesses (Dong and Yang, 2020).

3.2.3 Density of States

A density of states analysis examines the number of solution candidates with a certain fitness value. The density of states can tell us how likely it is to find a “good” solution via random search (Rosé et al., 1996). For example, a fitness landscape with many fitnesses near the global optimum will be relatively easy for random search.

3.2.4 Fitness Distance Correlations

One measure of problem difficulty is the correlation between distances to the nearest global optimum (in

²<https://github.com/D-X-Y/NATS-Bench>

our case, maximum) and the fitnesses of solution candidates. This correlation can help us measure the extent to which there is a “gradient” of fitness to a global optimum. One established metric is fitness distance correlation (FDC), which is a measure of problem difficulty for genetic algorithms (Jones et al., 1995). If we let F represent a list of fitnesses of \mathcal{S} and D represent the corresponding distances to the nearest global optimum, then the FDC is the Pearson correlation coefficient between F and D :

$$\text{FDC} = \frac{\text{cov}(F, D)}{\sigma_F \sigma_D}, \quad (2)$$

where $\text{cov}(F, D)$ is the covariance of F and D , and σ_F and σ_D are the standard deviations of F and D , respectively. In addition to FDC, we also examine Spearman and Kendall rank correlations between F and D . The Spearman fitness distance rank correlation is

$$\rho = \frac{\text{cov}(R(F), R(D))}{\sigma_{R(F)} \sigma_{R(D)}}, \quad (3)$$

where $R(F)$ and $R(D)$ are F and D converted to ranks, respectively. Then, the Kendall fitness distance rank correlation is

$$\tau = \frac{2}{n(n-1)} \sum_{i < j} \text{sgn}(f_i - f_j) \text{sgn}(d_i - d_j), \quad (4)$$

where $n = |\mathcal{S}| = |F| = |D|$ and f_i and d_i are the i th elements of F and D , respectively.

We clarify that while the Spearman and Kendall correlations are correlations between fitness and distance, the term “fitness distance correlation” or FDC specifically refers to Pearson’s correlation, as established in the literature (Jones et al., 1995).

3.2.5 Local Optima

A solution candidate x is a local optimum if it is the fittest among its neighborhood (Pitzer and Affenzeller, 2012):

$$\text{local optima}(x) \iff \forall y \in \mathcal{N}(x), f(x) > f(y). \quad (5)$$

We clarify that while this definition may sometimes be referred to as a *strict* local optimum, we use the term local optimum to be consistent with Pitzer and Affenzeller’s definitions. The number of local optima can tell us about the global ruggedness of a fitness landscape, for instance, a multi-modal landscape is more globally rugged than a unimodal one. Furthermore, correlations between local optima fitness and distance to a global optimum can tell us the extent to which there is a progression of fitness from local optima to a global optimum.

3.2.6 Basins of Attraction

Related to local optima is the concept of basins of attraction. Although the fitness landscape of NATS-Bench is a maximization problem, we use the term *basins of attraction* to remain consistent with the literature. To understand basins of attraction, we must first understand an *upward path* to a local maximum. We adapt this definition from the definition of a *downward path* by Pitzer et al. (Pitzer et al., 2010). An upward path p_\uparrow from candidate x_0 to x_n is the sequence $\{x_i\}_{i=0}^n$ where $(\forall i < j), f(x_i) \leq f(x_j), f(x_0) < f(x_n)$, and $x_{i+1} \in \mathcal{N}(x_i)$, that is, each solution candidate in the upward path is at least as fit as the previous one. Then, the weak basin of local optimum o is defined as

$$b(o) := \{x | x \in \mathcal{S}, p_\uparrow(x, o)\}, \quad (6)$$

which is the subset of the search space that has an upward path leading to o . A strong basin of a local optimum o is defined as

$$\hat{b}(o) := \{x | x \in b(o), (\nexists o' \neq o \in \mathcal{O}) \text{ with } x \in b(o')\} \quad (7)$$

where \mathcal{O} is the set of all local optima. In other words, the strong basin of a local optimum o is the subset of the search space that has an upward path only to o .

The relative fitnesses of the local optima combined with the relative sizes of their basins of attraction can indicate problem difficulty, as local optima with larger basins are more likely to be found via local search methods.

3.2.7 Neutral Networks

A neutral network is a set of connected solution candidates with equal fitness and can be intuitively described as a “plateau” of fitness (Pitzer and Affenzeller, 2012).

3.2.8 Autocorrelation and Correlation Length

Autocorrelation and correlation length are two measures for ruggedness of a fitness landscape (Weinberger, 1990). The autocorrelation function for some lag i is the Pearson correlation coefficient between a random walk on the landscape and the same walk with time delay i . Then for a random walk F_t and a lag i , the autocorrelation function is

$$\rho(i) = \frac{\text{cov}(F_t, F_{t+i})}{\sigma_{F_t} \sigma_{F_{t+i}}}. \quad (8)$$

where F_{t+i} is F_t with a lag of i , $\text{cov}(F_t, F_{t+i})$ is the covariance of F_t and F_{t+i} , and σ_{F_t} and $\sigma_{F_{t+i}}$ are the standard deviations of F_t and F_{t+i} , respectively. Correlation length is defined as $\tau = \frac{-1}{\ln|\rho(1)|}$ for $\rho(1) \neq 0$,

which is the expected distance between points before they become “uncorrelated” (Weinberger, 1990; Tavares et al., 2008).

4 RESULTS

We compare the difficulty and shape of the NATS-Bench topology search space for three different fitness landscapes of CIFAR-10, CIFAR-100, and ImageNet16-120 test accuracies. We calculate, analyze, and visualize characteristics of density of states, FDC and fitness distance rank correlations, local optima, basins of attraction, neutral networks, and autocorrelation. Our analysis could indicate that the problem difficulty for the NAS search problems correspond to the difficulties of the image classification problems themselves, with the nuance that the use of different metrics results in different orderings of difficulty for the three fitness landscapes.

While analyses of larger search spaces may need to use sampling to approximate fitness landscape characteristics (Nunes et al., 2021; Traoré et al., 2021), \mathcal{S}_i in NATS-Bench is relatively small, so we are able to exhaustively evaluate the search space for most of our metrics. To estimate autocorrelation, we average 200 random walks of length 100 on the search space with random starting points. Our data and code are publicly available online.³

4.1 Density of States

As seen in Figure 3, CIFAR-10 has the most architectures near the global optimum, followed by CIFAR-100, then ImageNet16-120. This may indicate that NAS on architectures for CIFAR-10 image classification is the easiest, followed by CIFAR-100 and lastly ImageNet16-120. This order of difficulty for the NATS-Bench fitness landscapes matches the order of difficulty for the image classification problems themselves. Our density of states analysis of the NATS-Bench topology space test accuracies is consistent with Ochoa and Veerapen’s analysis of the validation accuracies.

4.2 Fitness Distance Correlations

FDC can be used to characterize problem difficulty for genetic algorithms and can divide problems into three broad categories. $FDC \geq 0.15$ is considered *misleading*, because solution candidates decrease in fitness as they approach a global optimum. $-0.15 <$

³<https://github.com/v-tao/nats-bench-landscape>

Table 1: Correlations between architecture fitness and distance to the global optimum.

| | CIFAR-10 | CIFAR-100 | ImageNet |
|--------|----------|-----------|----------|
| FDC | -.2199 | -.3090 | -.3163 |
| ρ | -.4144 | -.4666 | -.3270 |
| τ | -.3200 | -.3630 | -.2502 |

$FDC < 0.15$ is *difficult* because there is weak to no correlation between fitnesses and distances to the global optimum, and $FDC \leq -0.15$ is *straightforward*, as solution candidates approaching the global optimum increase in fitness (Jones et al., 1995). From the rank correlations in Table 1, the CIFAR-100 landscape appears the most straightforward, followed by CIFAR-10 and then ImageNet16-120, which is consistent with Ochoa and Veerapen’s analyses. However, examining FDC which is Pearson’s correlation, the ImageNet16-120 landscape appears the most straightforward, followed by CIFAR-100 and then CIFAR-10. Thus, we demonstrate how different metrics can cause different interpretations of problem difficulty.

4.3 Local Optima

Table 2: Correlations between architecture fitness and distance to global optimum of local optima.

| | CIFAR-10 | CIFAR-100 | ImageNet |
|----------|----------|-----------|----------|
| # optima | 17 | 24 | 36 |
| FDC | -.8741 | -.8225 | -.6172 |
| ρ | -.8650 | -.7916 | -.6311 |
| τ | -.7223 | -.6845 | -.5050 |

For the test accuracies, ImageNet16-120 has the most local optima, followed by CIFAR-100 and CIFAR-10 (see Table 2), corroborating Ochoa and Veerapen’s modality analysis of the validation accuracies. In contrast to the whole search space, which has a weak negative correlation between fitness and distance to the global optimum (see Table 1 and Figure 4), the subset of just local optima has a strong negative correlation between these features, as seen in Table 2 and Figure 5. This suggests there is a progression of fitnesses from local optima to the global optimum for all three fitness landscapes.

4.4 Basins of Attraction

From Table 3, we see that for each fitness landscape, the vast majority of the search space is in a weak basin of attraction, meaning almost any starting architecture can reach a local optimum via local search. Combined with Figure 5, this demonstrates that search on \mathcal{S}_i for CIFAR-10 is easy, as the local optima for CIFAR-10

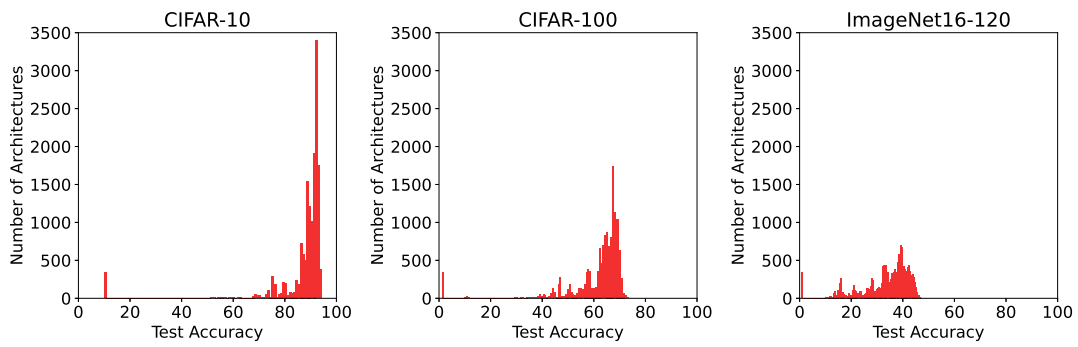


Figure 3: Density of states of NATS-Bench topology search space test accuracies. The maximum fitness for each fitness landscape is 94.37, 73.51, and 47.31 for CIFAR-10, CIFAR-100, and ImageNet16-120, respectively.

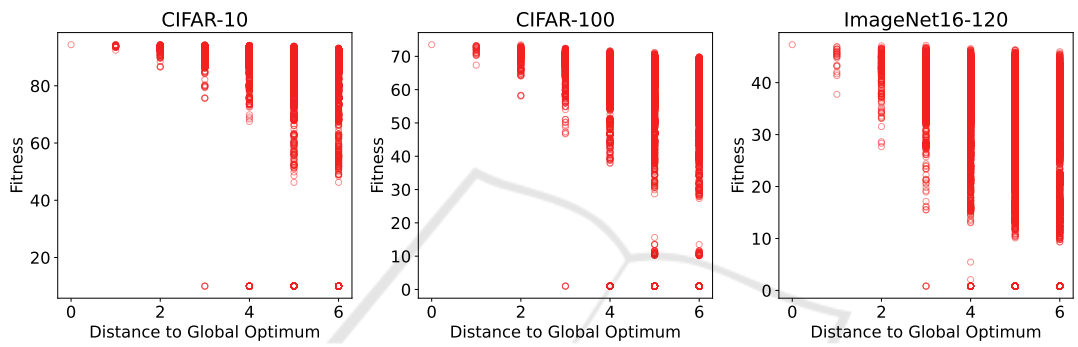


Figure 4: Fitness vs. distance to the global optimum.

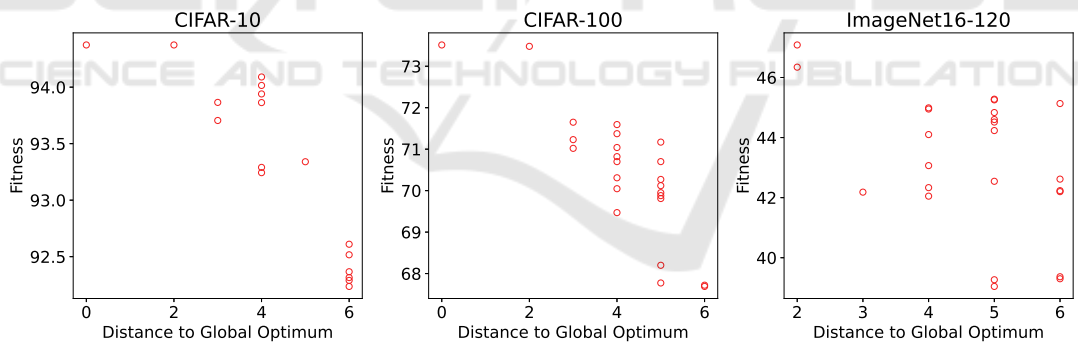


Figure 5: Fitness vs. distance to the global optimum for local optima.

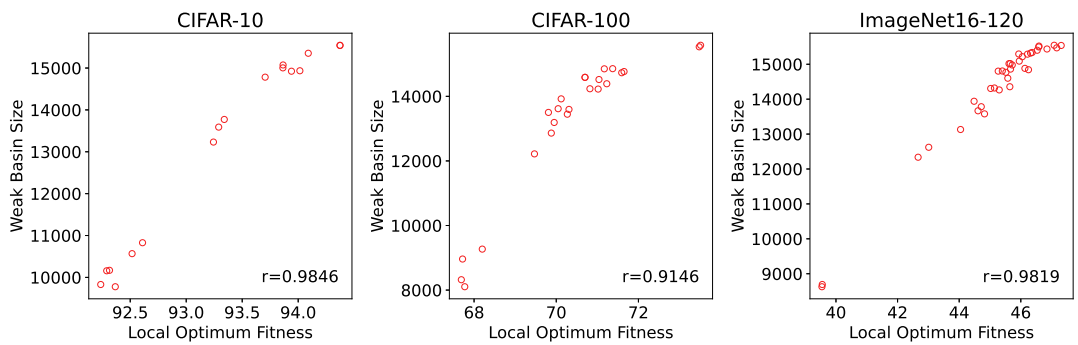


Figure 6: Fitness vs. size of weak basin for local maxima.

Table 3: Summary statistics of weak basins of attraction.

| | CIFAR-10 | CIFAR-100 | ImageNet |
|-----------|----------|-----------|----------|
| # basins | 17 | 24 | 36 |
| Avg. size | 13122.06 | 13245.08 | 14337.81 |
| Extent | .9989 | .9984 | .9977 |

Table 4: Summary statistics of strong basins of attraction.

| | CIFAR-10 | CIFAR-100 | ImageNet |
|-----------|----------|-----------|----------|
| # basins | 4 | 8 | 14 |
| Avg. size | 10.00 | 7.88 | 2.29 |
| Extent | .0026 | .0040 | .0020 |

are close in fitness to the global optimum. While the ranges in local optima fitness are greater for CIFAR-100 and ImageNet16-120, all three fitness landscapes show a strong correlation between local optima fitness and weak basin extent. This may also indicate problem easiness, as fitter optima are more likely to be achieved via local search.

4.5 Neutral Networks

Table 5: Neutral network summary statistics.

| | CIFAR-10 | CIFAR-100 | ImageNet |
|-----------|----------|-----------|----------|
| # nets | 249 | 35 | 46 |
| Avg. size | 3.41 | 7.46 | 5.41 |
| Max. size | 341 | 63 | 67 |

Only a small fraction ($< .01$) of the search space belongs to a neutral network (see Table 5). From Figure 7, we observe most neutral networks contain only a handful of architectures and are the worst-performing architectures in the search space. These architectures correspond to the “spikes” on the left of each histogram in Figure 3.

Close inspection of the largest neutral network in each fitness landscape reveals that these neutral networks consist entirely of architectures where the input node and output node are disconnected, resulting in an architecture that performs equal to random choice. In some cases, large neutral networks may be beneficial because they allow exploration of a large space while maintaining the same fitness (Pitzer et al., 2010; Wagner, 2008). Although our data in Table 6 indicate that exploring these neutral networks do provide access to genetic diversity, these neutral networks consist of the worst architectures in the search space, so it may not be desirable to remain in these neutral networks over many iterations.

4.6 Autocorrelation

The correlation lengths are 1.53, 1.71, and 2.23 for CIFAR-10, CIFAR-100, and ImageNet16-120, respectively. Furthermore, we can see from Figure 8 that the autocorrelation function for ImageNet16-120 decays slower than for CIFAR-10 or CIFAR-100. Both the correlation length and the autocorrelation function indicate that at the local level, ImageNet16-120 is the smoothest out of the three fitness landscapes.

5 DISCUSSION

Our fitness landscape analyses could indicate that the difficulties associated with the three fitness landscapes of CIFAR-10, CIFAR-100, and ImageNet16-120 on the NATS-Bench topology search space correspond to the difficulties of the image classification problems themselves. This is reflected in the density of states, as CIFAR-10 has the greatest proportion of architectures close to the global optimum, followed by CIFAR-100 and ImageNet16-120. In addition, while all three fitness landscapes have similar weak and strong basin extents, both the number of local optima and the range of fitness values for local optima is smallest for CIFAR-10, then CIFAR-100, then ImageNet16-120. This means that for CIFAR-10, not only is the global optimum more likely to be reached via local search, but also any local optimum reached is closer in fitness to the global optimum than for the other two fitness landscapes. Previous work indicates that ImageNet16-120 is the most difficult for validation accuracies of \mathcal{S}_v (Ochoa and Veerapen, 2022), and our work shows a similar case for the test accuracies.

However, our data contains some discrepancies which would at first appear to be contradictions. The progression of difficulty from CIFAR-10 to ImageNet16-120 is not supported by our data on correlations between architecture fitness and distance to the global optimum. By FDC, ImageNet16-120 is the most straightforward, while the rank correlations point to CIFAR-100 as the most straightforward. We can resolve this discrepancy by considering the different algorithms that may be applied to the optimization problem. As FDC is a measure of problem difficulty for genetic algorithms (Jones et al., 1995), the lowest FDC may indicate that ImageNet16-120 is the most straightforward for a genetic algorithm whereas the lowest rank correlation may indicate that CIFAR-100 is the most straightforward for algorithms like hill climbing that only use relative fitness values.

Previous work has used number of local op-

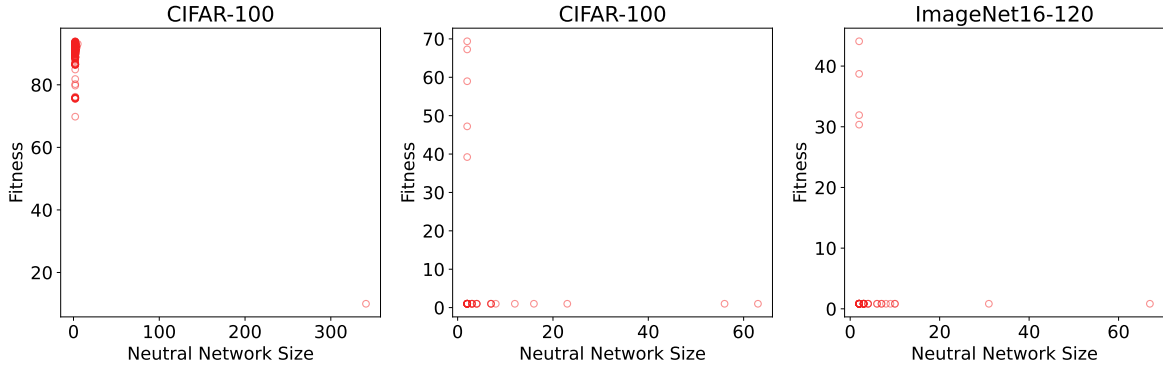


Figure 7: Fitness vs. size of neutral networks.

Table 6: Properties of largest neutral network and its neighbors.

| | CIFAR-10 | CIFAR-100 | ImageNet |
|----------------------------|----------|-----------|----------|
| Size | 341 | 63 | 67 |
| Fitness | 10.00 | 1.00 | .83 |
| Max. edit distance | 6 | 6 | 6 |
| Avg. edit distance | 4.8031 | 4.8249 | 4.8318 |
| Unique phenotypes | 5 | 5 | 5 |
| Unique neighbor genotypes | 2868 | 917 | 974 |
| Unique neighbor phenotypes | 513 | 177 | 182 |

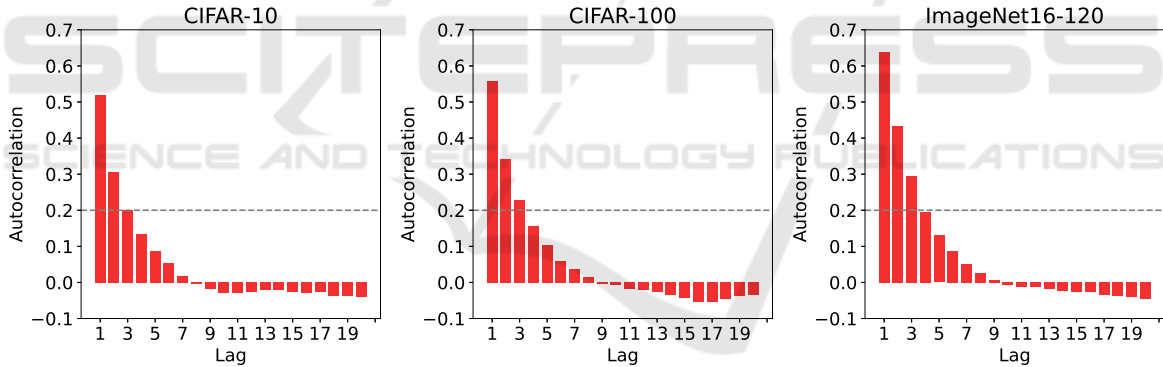


Figure 8: Autocorrelation functions sampled from 200 random walks of length 100.

tima to describe the ruggedness of the NATS-Bench topology fitness landscapes (Ochoa and Veerapen, 2022). While our own analysis of local optima support these claims of ruggedness, we should be more careful in describing this as *global* ruggedness. As ImageNet16-120 has the most local optima, followed by CIFAR-100 and CIFAR-10, ImageNet16-120 appears the most rugged on a global level. However, our autocorrelation and correlation length analyses point to the reverse order of ruggedness on a *local* level. These discrepancies demonstrate that the fitness landscape of an NAS search problem is multi-faceted, and many metrics are required to paint a fuller picture of the NAS fitness landscape. Furthermore, a fitness

landscape analysis should be done with nuance, and consider the different implications of metrics for different algorithms.

Our fitness landscape analysis contributes to a growing body of work aimed at combining evolutionary computation and explainable AI. As an intersection between explainable AI and NAS, our work directly addresses a challenge mentioned by Bacardit et al.’s recent position paper on the subject (Bacardit et al., 2022). With the rise in popularity of NAS, we illustrate how evolutionary computation methods can contribute to understanding NAS search spaces.

6 CONCLUSION

We performed a fitness landscape analysis of the NATS-Bench topology search space, analyzing and visualizing features of density of states, FDC and fitness distance rank correlations, local optima, basins of attraction, neutral networks, and autocorrelation. Our analyses indicated that the problem difficulty of search on the topology search space of NATS-Bench for architectures that can perform well on CIFAR-10, CIFAR-100, and ImageNet16-120 datasets may correspond to the difficulties of the image classification problems themselves. We also demonstrated the importance of multiple metrics and nuance in the interpretation of an NAS fitness landscape.

While these metrics can help to characterize the fitness landscape, ultimately they are not exact. Future work may include the comparison of different algorithms on NATS-Bench in order to discern how useful these metrics are for describing the true fitness landscape of NATS-Bench. As our current understanding of NAS search spaces is limited, future work may also include fitness landscape analyses of other NAS search spaces, such as non-tabular search spaces (Siems et al., 2020) or for problems other than image classification (Klyuchnikov et al., 2022; Mehrotra et al., 2020). Another possible direction is to investigate what properties of the architectures themselves cause the fitness landscapes to appear this way.

REFERENCES

- Abdel-Hamid, O., Mohamed, A.-r., Jiang, H., Deng, L., Penn, G., and Yu, D. (2014). Convolutional neural networks for speech recognition. *IEEE/ACM Transactions on audio, speech, and language processing*, 22(10):1533–1545.
- Bacardit, J., Brownlee, A. E., Cagnoni, S., Iacca, G., McCall, J., and Walker, D. (2022). The intersection of evolutionary computation and explainable ai. In *Proceedings of the Genetic and Evolutionary Computation conference companion*, pages 1757–1762.
- Chen, W., Gong, X., and Wang, Z. (2021). Neural architecture search on imagenet in four gpu hours: A theoretically inspired perspective. *arXiv preprint arXiv:2102.11535*.
- Chitty-Venkata, K. T., Emani, M., Vishwanath, V., and Somani, A. K. (2023). Neural architecture search benchmarks: Insights and survey. *IEEE Access*, 11:25217–25236.
- Chrabaszcz, P., Loshchilov, I., and Hutter, F. (2017). A downsampled variant of imagenet as an alternative to the cifar datasets. *arXiv preprint arXiv:1707.08819*.
- Dong, X., Liu, L., Musial, K., and Gabrys, B. (2021). Nats-bench: Benchmarking nas algorithms for architecture topology and size. *IEEE transactions on pattern analysis and machine intelligence*, 44(7):3634–3646.
- Dong, X. and Yang, Y. (2019). One-shot neural architecture search via self-evaluated template network. In *Proceedings of the IEEE/CVF International Conference on Computer Vision*, pages 3681–3690.
- Dong, X. and Yang, Y. (2020). Nas-bench-201: Extending the scope of reproducible neural architecture search. *arXiv preprint arXiv:2001.00326*.
- Guo, Z., Zhang, X., Mu, H., Heng, W., Liu, Z., Wei, Y., and Sun, J. (2020). Single path one-shot neural architecture search with uniform sampling. In *Computer Vision—ECCV 2020: 16th European Conference, Glasgow, UK, August 23–28, 2020, Proceedings, Part XVI 16*, pages 544–560. Springer.
- He, K., Zhang, X., Ren, S., and Sun, J. (2016). Deep residual learning for image recognition. In *Proceedings of the IEEE conference on computer vision and pattern recognition*, pages 770–778.
- Jones, T., Forrest, S., et al. (1995). Fitness distance correlation as a measure of problem difficulty for genetic algorithms. In *ICGA*, volume 95, pages 184–192.
- Klyuchnikov, N., Trofimov, I., Artemova, E., Salnikov, M., Fedorov, M., Filippov, A., and Burnaev, E. (2022). Nas-bench-nlp: neural architecture search benchmark for natural language processing. *IEEE Access*, 10:45736–45747.
- Krizhevsky, A. and Hinton, G. (2009). Learning multiple layers of features from tiny images. Technical Report 0, University of Toronto, Toronto, Ontario.
- Krizhevsky, A., Sutskever, I., and Hinton, G. E. (2012). Imagenet classification with deep convolutional neural networks. *Advances in neural information processing systems*, 25.
- Li, L. and Talwalkar, A. (2020). Random search and reproducibility for neural architecture search. In *Uncertainty in artificial intelligence*, pages 367–377. PMLR.
- Liu, H., Simonyan, K., and Yang, Y. (2018). Darts: Differentiable architecture search. *arXiv preprint arXiv:1806.09055*.
- Mehrotra, A., Ramos, A. G. C., Bhattacharya, S., Dudziak, Ł., Vipplerla, R., Chau, T., Abdelfattah, M. S., Ishtiaq, S., and Lane, N. D. (2020). Nas-bench-asr: Reproducible neural architecture search for speech recognition. In *International Conference on Learning Representations*.
- Mellor, J., Turner, J., Storkey, A., and Crowley, E. J. (2021). Neural architecture search without training. In *International Conference on Machine Learning*, pages 7588–7598. PMLR.
- Merz, P. and Freisleben, B. (2000). Fitness landscape analysis and memetic algorithms for the quadratic assignment problem. *IEEE Transactions on Evolutionary Computation*, 4(4):337–352.
- Nunes, M., Fraga, P. M., and Pappa, G. L. (2021). Fitness landscape analysis of graph neural network architecture search spaces. In *Proceedings of the Genetic and Evolutionary Computation Conference*, pages 876–884.

- Ochoa, G. and Veerapen, N. (2022). Neural architecture search: a visual analysis. In *International Conference on Parallel Problem Solving from Nature*, pages 603–615. Springer.
- Pitzer, E. and Affenzeller, M. (2012). A comprehensive survey on fitness landscape analysis. *Recent advances in intelligent engineering systems*, pages 161–191.
- Pitzer, E., Affenzeller, M., and Beham, A. (2010). A closer look down the basins of attraction. In *2010 UK workshop on computational intelligence (UKCI)*, pages 1–6. IEEE.
- Potgieter, I., Cleghorn, C. W., and Bosman, A. S. (2022). A local optima network analysis of the feedforward neural architecture space. In *2022 International Joint Conference on Neural Networks (IJCNN)*, pages 1–8. IEEE.
- Rodrigues, N. M., Malan, K. M., Ochoa, G., Vanneschi, L., and Silva, S. (2022). Fitness landscape analysis of convolutional neural network architectures for image classification. *Information Sciences*, 609:711–726.
- Rodrigues, N. M., Silva, S., and Vanneschi, L. (2020). A study of generalization and fitness landscapes for neuroevolution. *IEEE Access*, 8:108216–108234.
- Rosé, H., Ebeling, W., and Asselmeyer, T. (1996). The density of states — a measure of the difficulty of optimisation problems. In Voigt, H.-M., Ebeling, W., Rechenberg, I., and Schwefel, H.-P., editors, *Parallel Problem Solving from Nature — PPSN IV*, pages 208–217. Berlin, Heidelberg. Springer Berlin Heidelberg.
- Sheikhtaheri, A., Sadoughi, F., and Hashemi Dehaghi, Z. (2014). Developing and using expert systems and neural networks in medicine: a review on benefits and challenges. *Journal of medical systems*, 38:1–6.
- Siems, J., Zimmer, L., Zela, A., Lukasik, J., Keuper, M., and Hutter, F. (2020). Nas-bench-301 and the case for surrogate benchmarks for neural architecture search. *arXiv preprint arXiv:2008.09777*, 4:14.
- Stanley, K. O., Clune, J., Lehman, J., and Miikkulainen, R. (2019). Designing neural networks through neuroevolution. *Nature Machine Intelligence*, 1(1):24–35.
- Szegedy, C., Toshev, A., and Erhan, D. (2013). Deep neural networks for object detection. *Advances in neural information processing systems*, 26.
- Tavares, J., Pereira, F. B., and Costa, E. (2008). Multi-dimensional knapsack problem: A fitness landscape analysis. *IEEE Transactions on Systems, Man, and Cybernetics, Part B (Cybernetics)*, 38(3):604–616.
- Thomson, S. L., Ochoa, G., Veerapen, N., and Michalak, K. (2023). Channel configuration for neural architecture: Insights from the search space. In *Proceedings of the Genetic and Evolutionary Computation Conference*, pages 1267–1275.
- Traoré, K. R., Camero, A., and Zhu, X. X. (2021). Fitness landscape footprint: A framework to compare neural architecture search problems. *arXiv preprint arXiv:2111.01584*.
- Wagner, A. (2008). Robustness and evolvability: a paradox resolved. *Proceedings of the Royal Society B: Biological Sciences*, 275(1630):91–100.
- Weinberger, E. (1990). Correlated and uncorrelated fitness landscapes and how to tell the difference. *Biological cybernetics*, 63(5):325–336.
- White, C., Safari, M., Sukthanker, R., Ru, B., Elsken, T., Zela, A., Dey, D., and Hutter, F. (2023). Neural architecture search: Insights from 1000 papers. *arXiv preprint arXiv:2301.08727*.
- Wright, S. et al. (1932). The roles of mutation, inbreeding, crossbreeding, and selection in evolution. *Proceedings of the Sixth International Congress of Genetics*.
- Ying, C., Klein, A., Christiansen, E., Real, E., Murphy, K., and Hutter, F. (2019). Nas-bench-101: Towards reproducible neural architecture search. In *International conference on machine learning*, pages 7105–7114. PMLR.
- Zoph, B. and Le, Q. V. (2016). Neural architecture search with reinforcement learning. *arXiv preprint arXiv:1611.01578*.